Iron-silicon alloy in Earth's core?

Jung-Fu Lin[*,i], Dion L. Heinz[*,†], Andrew J. Campbell[*], James M. Devine[*], Guoyin Shen[‡]

[*]Department of the Geophysical Sciences, The University of Chicago, Chicago, IL 60637

[†]Also at the James Franck Institute, The University of Chicago, Chicago, IL 60637

[‡]Consortium for Advanced Radiation Sources, The University of Chicago, Chicago, IL 60637

[i]email address: afu@geosci.uchicago.edu

We have investigated the phase relations in the iron-rich portion of the Fe-Si alloys at high pressures and temperatures. Our study indicates that Si alloyed with Fe can stabilize the bcc phase up to at least 84 GPa (compared to ~10 GPa for pure Fe) and 2400 K. Earth's inner core may be composed of hcp Fe with up to 4 wt% Si, but it is also conceivable that the inner core could be a mixture of a Si-rich bcc phase and a Si-poor hcp phase.

Iron is the most abundant element in Earth's core. However, the density of the outer core is about 10% lower than the density of Fe at the pressure and temperature conditions of the outer core, indicating the presence of a low-atomic-weight component (such as H, C, O, Si, and S) in the core (1). There is also evidence that the inner core may be less dense than pure Fe, and the amount of light elements in the inner core may be about 0-3 wt% (2-4). Silicon may be an important alloying element in the outer core, based on its cosmochemical abundance and its measured thermoelastic properties (5, 6). Silicon was excluded as the primary alloying element in the outer core based on the equation of state (EOS) of the intermediate compound ε-FeSi (7). However, studying the Fe-rich portion of the Fe-Si system is more appropriate for understanding the possible effect of Si on the EOS and the crystal structure of Fe under core conditions. The phase diagram of Fe has been extensively studied; body-centered cubic (bcc) Fe transforms to the hexagonal

close-packed (hcp) phase under high pressures, and the bcc phase transforms to the face-centered cubic (fcc) phase under high temperatures (8). In situ x-ray diffraction studies to 161 GPa and 3000 K demonstrate that hcp-Fe has a wide stability field extending from the deep mantle to core conditions (9). We studied the Fe-rich portion of the Fe-Si alloys in order to understand the possible crystal structures and the phase diagram relevant to the Earth's core.

The Fe7.9wt%Si alloy was studied in a laser-heated diamond anvil cell (LHDAC) at pressures up to 84 GPa and temperatures up to 2400 K, and x-ray diffraction patterns were collected in situ (see Web Fig. 1, 10) (11). The bcc phase transformed to the bcc+hcp phases at 16 GPa and 300 K, and the phase transformation to the hcp phase was completed at 36 GPa. When laser heated below 16 GPa, the bcc phase transformed to a mixture of bcc+fcc phases. The hcp phase transformed to bcc+hcp phases under high temperatures and, upon further heating, bcc+hcp phases transformed to bcc+fcc phases (Fig. 1). Upon pressure quench, the sample reverted to the bcc phase. The quenched samples from a LHDAC were then analyzed with a scanning electron microprobe (SEM), and the results indicate that the starting material decomposed into two chemical compositions at high pressure and temperature; the bcc phase was presumably enriched in Si, and the coexisting hcp or fcc phase was depleted in Si relative to the starting composition (Fig. 2). The partitioning of Si between bcc and hcp phases or between bcc

and fcc phases indicates the presence of two-phase equilibria under high pressure and temperature (P-T) conditions. Compared to the phase diagram of pure Fe (8), it is evident that the stability field of the bcc phase can be extended to higher pressures and temperatures with the addition of Si (Fig. 1). A Fe2.2wt%Si alloy was also studied in a LHDAC. This lower amount of alloying Si did not have a strong effect on the phase diagram of Fe; hcp-Fe2.2wt%Si transformed entirely to the fcc phase while laser heated at about 34 GPa to 1400 K.

To better understand the T-composition (X) phase diagram of Fe-Si alloys at high pressure, we also conducted in situ x-ray experiments, along with chemical analyses of the quenched samples, on Fe4.0wt%Si and Fe7.9wt%Si in a large-volume press (LVP) and a LHDAC (17) at about 16 GPa (Fig. 2; see Web Fig. 2, 20). Three regions of the two-phase equilibria are observed: bcc+hcp, bcc+fcc, and hcp+fcc. As shown, adding Si into Fe can change the phase diagram of Fe; the hcp to fcc phase transformation at lower Si contents becomes a more complicated phase transition sequence at higher Si contents (Fig. 3). The maximum solubility of Si in the fcc phase at zero pressure is only 1.9 wt% (21), but the effect of pressure increases the solubility of Si in the fcc phase to over 6 wt% at 16 GPa (22) (Table 1).

Sulfur and oxygen are also considered to be two possible light elements in the core, and the properties of FeS and FeO under high pressures and temperatures have been

frequently used to discuss the possibility of sulfur and oxygen in the core (3). Although the solubility of oxygen in Fe is low at ambient pressure, high-pressure experiments on the Fe-FeO system have shown that oxygen is soluble in Fe at high P-T conditions (23). The phase of FeS known at the highest P-T conditions has the hexagonal NiAs structure, suggesting that S may also form solid solution with Fe under core conditions (24). As demonstrated in the Fe-Si alloy experiments reported here, a small alloying component can have a large effect on the phase diagram. Since the physical properties of the liquid often mimic the properties of the corresponding solids, it is likewise possible that adding a small alloying component to liquid Fe may also have a significant effect on the liquid structure of Fe (25).

Our results show that a light element alloyed with iron can change the topology of the subsolidus phase diagram of iron under high P-T conditions. Adding Si into Fe stabilizes the bcc phase to much higher pressures and temperatures. However, only 2-4 wt% Si is not enough to change the phase diagram of Fe (Fig. 3). Therefore, if the inner core only contains 2-4 wt% of Si, then it is likely to have the hcp structure. It is also conceivable that the inner core could be a mixture of a Si-rich bcc phase and a Si-poor hcp phase. The existence of two phases with different compositions may influence interpretation of the observed seismic anisotropy of the inner core (26, 27).

References:

1. F. Birch, *J. Geophys. Res.* **69**, 4377 (1964).

2. L. Stixrude, E. Wasserman, R. E. Cohen, *J. Geophys. Res.* **102**, 24729 (1997).

3. V. J. Hillgren, C. K. Gessmann, J. Li, in *Origin of the Earth and the Moon,* R. M. Canup, K. Righter, Eds. (The University of Arizona Press, Arizona, 2000) pp. 256.

4. H. K. Mao et al., *Science* **292**, 914 (2001).

5. A. S. Balchan, G. R. Cowan, *J. Geophys. Res.* **71**, 3577 (1966).

6. J. Zhang, F. Guyot, *Phys. Chem. Minerals* **26**, 206 (1999).

7. E. Knittle, Q. Williams, *Geophys. Res. Lett.* **22**, 445 (1995).

8. G. Shen, H. K. Mao, R. J. Hemley, T. S. Duffy, M. L. Rivers, *Geophys. Res. Lett.* **25**, 373 (1998).

9. R. Hemley, H. K. Mao, *Int. Geol. Rev.* **43**, 1 (2001).

10.

11. The starting materials, Fe2.2wt%Si, Fe4.0wt%Si, and Fe7.9wt%Si alloys in the bcc structure, were obtained from Goodfellow Corporation and Prof. William Bassett at Cornell University and were analyzed with an electron microprobe. The sample was grounded into fine powder (~1 μm in grain size) and pre-compressed with a diamond anvil cell (DAC) to make a thin, flat disk. A stainless steel or rhenium gasket was pre-indented to a thickness of 25 μm and then a hole of 100 μm diameter was drilled in it. The diameter of the sample in a DAC was about 50 μm and the thickness was about 10

μm. A sandwiched sample configuration, using NaCl, MgO, or Ar as the thermal insulator and pressure medium, was used in this study (12). When NaCl or MgO was used as the thermal insulator, water contamination was eliminated by heating the DAC in a vacuum oven at 100 ˚C for an hour before sealing the cell. The different pressure media were used to demonstrate that our results were independent of the pressure media.

A double-sided Nd:YLF laser heating system, operating in donut mode (TEM_{01}) or in multimode (TEM_{00}+TEM_{01}), was used to laser heat the sample from both sides of a DAC at the GSECARS sector of the Advanced Photon Source (APS), Argonne National Laboratory (ANL) (12). The laser beam diameter was about 25 μm. Alignment of the laser with the x-ray beam exploited the x-ray induced fluorescence of the insulating pressure media. Temperatures were measured spectroradiometrically; greybody temperatures were determined by fitting the thermal radiation spectrum between 670 nm and 830 nm to the Planck radiation function (12). The laser power and the thermal radiation from the laser heated sample were used to stabilize the temperatures in most of the experiments. The sample was laser heated for one to five minutes at a target temperature, and at least three thermal radiation spectra were taken for the temperature measurement. The temperature uncertainty (1σ) averaged from multiple temperature measurements and temperatures from both sides of the sample across the laser heated spots was 50 K to 150 K in most of the experiments. A white beam or a monochromatic

beam (wavelength = 0.4246 Å) was used as the x-ray source, for either energy-dispersive x-ray diffraction (EDXRD) or angle-dispersive x-ray diffraction (ADXRD), respectively. The synchrotron x-ray beam was about 8 μm in diameter. The diffracted x-rays were collected by a germanium detector at a fixed angle (2θ) of about 8˚ in EDXRD, or by a CCD in ADXRD. All diffraction lines were identified as either sample, pressure standard, pressure medium, or gasket. Pressures were calculated from the room temperature EOS of NaCl (13, 14) or MgO (15), or by the ruby fluorescence pressure scale (16) in the Ar medium before laser heating. No thermal pressure corrections were made to the pressures at high temperatures.

12. G. Shen, M. L. Rivers, Y. Wang, S. R. Sutton, *Rev. Sci. Instrum.* **72**, 1273 (2001).

13. F. Birch, *J. Geophys. Res.* **91**, 4949 (1986).

14. D. L. Heinz, R. Jeanloz, *Phys. Rev. B* **30**, 6045 (1984).

15. S. Speziale, C. S. Zha, T. S. Duffy, R. Hemley, H. K. Mao, *J. Geophys. Res.* **106**, 515 (2001).

16. H. K. Mao, J. Xu, P. M. Bell, *J. Geophys. Res.* **91**, 4673 (1986).

17. In situ x-ray experiments on the Fe-Si alloys were conducted in a 250 ton large volume press (LVP) installed at the 13-BMD beamline, GSECARS, APS. The “T-cup” multi-anvil apparatus, consisting of eight cube-shaped anvils (10 mm edge length) made of tungsten carbide with truncated edge length of 2 mm, was used in this study (18). Both

the starting materials (Fe4.0wt%Si or Fe7.9wt%Si alloy) and the pressure calibrant (Au) (19) were mixed with MgO powder to prevent grain growth. The sample and the pressure calibrant were packed in separate layers in the sample chamber which was made of a mixture of amorphous boron and epoxy resin. A $W_{0.94}Re_{0.06}$-$W_{0.75}Re_{0.25}$ thermocouple was located at the center of the sample chamber for measuring the temperature. A mixture of TiC and diamond powder (1:1 by weight) was used as the internal heater, and $LaCrO_3$ semi-sintered plates were used as thermal insulation to prevent heat loss. A white beam was used as the x-ray source, and the diffracted x-rays were collimated to 100 μm x 300 μm by slits and collected by a germanium detector at a fixed angle (2θ) of about 6˚. x-ray diffraction patterns were taken for phase identification while the sample was under high P-T conditions. Quenched samples were carefully recovered, polished, carbon-coated, and then analyzed with a SEM. No reaction between MgO and the Fe-Si alloys was observed in x-ray diffraction experiments and in a SEM.

18. Y. Wang, M. Rivers, S. Sutton, P. Eng, *Rev. High Pressure Sci. Technol.* **7**, 1490 (1998).

19. D. L. Heinz and R. Jeanloz, *J. Appl. Phys*. **55**, 885 (1984).

20.

21. O. Kubaschewski, *Iron-Binary phase diagrams* (Springer-Verlag, New York, 1982).

22. J. Zhang, F. Guyot, *Phys. Chem. Minerals* **26**, 419 (1999).

23. A. E. Ringwood, W. Hibberson, *Phys. Chem. Minerals* **17**, 313 (1990).

24. Y. Fei, C. T. Prewitt, H. K. Mao, C. M. Bertka, *Science* **268**, 1892 (1995).

25. C. Sanloup, et al., *Europhys. Lett.* **52**, 151 (2000).

26. J. Tromp, *Annu. Rev. Earth Planet. Sci.*, **29**, 47 (2001).

27. G. Steinle-Neumann, L. Stixrude, R. E. Cohen, O. Gulseren, *Nature*, **413**, 57 (2001).

28. The experiments were carried out at the William M. Keck High Pressure Laboratory at the GSECARS sector of the APS, ANL. We thank Prof. William Bassett for providing Fe-Si alloys, Dr. Andrew Davis, Dr. Ian Steele, and Dr. Steven Simon for their help with the chemical analyses, and Dr. Uchida Takeyuki and Sutatcha Hongsresawat for their help with LVP experiments. We also thank two anonymous reviewers, Dr. Linda Rowan, Dr. Mark Rivers, and Dr. Stephen Sutton for helpful comments. This research is supported by National Science Foundation grant EAR-9974373 and National Aeronautics and Space Administration grant NAG 5-9800 (A.C.) to Dr. Munir Humayun.

Table 1. Chemical analyses of the quenched Fe-Si samples. The measured Si contents were averaged from at least three analyses. Numbers in parentheses represent the standard deviation. These results indicate the width of the bcc+fcc or the bcc+hcp phases at the specific P-T conditions.

Run #	P (GPa)	T (K)	Starting materials	bcc (Si wt%)	fcc (Si wt%)	hcp (Si wt%)	Remarks
T0250	9.4	1200 (10)	Fe7.9wt%Si	11.44 (0.13)	5.32 (0.09)		LVP; x-ray
T0258	14.1	1100 (10)	Fe7.9wt%Si	10.30 (0.08)	6.71 (0.07)		LVP; x-ray
Fe9Si#17	14.2	1501 (105)	Fe7.9wt%Si	9.42 (0.11)	5.93 (0.09)		LHDAC*
Fe9Si#18	13.9	1387 (38)	Fe7.9wt%Si	9.82 (0.12)	5.91 (0.09)		LHDAC*
Fe9Si#11	30.6	1976 (69)	Fe7.9wt%Si	11.33 (0.22)	7.19 (0.18)		LHDAC; x-ray
Fe9Si#15	42.2	1804 (17)	Fe7.9wt%Si	10.92 (0.12)		7.69 (0.10)	LHDAC*

* indicates that Figure 1 was used for the phase identification for experiments that were conducted without x-ray.

Figure Captions:

Figure 1. Phases observed in LHDAC experiments with the starting materials of Fe7.9wt%Si. Green open diamonds: bcc only; blue open circles: hcp only; red open triangles: fcc+bcc; brown crosses: bcc+hcp; black rectangular dots: bcc+hcp+fcc; grey dashed curve: phase transformation from hcp to bcc+hcp; grey dashed curve with dots: phase transformation from bcc+hcp to fcc+bcc; solid grey lines: the phase diagram of iron (8). The slope of the phase transformation from hcp to bcc+hcp decreases with increasing pressure. Mixed phases are commonly observed in the heating process, indicating broad regions of two phase equilibria between bcc+hcp and bcc+fcc phases. The coexistence of the bcc+hcp+fcc phases may be due to the thermal gradient, temperature fluctuation, or slight misalignment of the laser beam with respect to the x-ray beam in the LHDAC.

Figure 2. Back-scattered electron image of the quenched LHDAC sample from 31 GPa and 1976 K. The laser beam was about 20 μm. The average Si concentration is 11.3 ($\pm$0.3) wt% in dark areas (bcc phase) and is about 7.2 ($\pm$0.1) wt% in bright areas (fcc phase), while the average Si concentration remains at about 8.1 ($\pm$0.2) wt% in the surrounding unheated area. The black bar on the picture is 10 μm.

Figure 3. Schematic T-X phase diagram (grey dashed lines) of iron-rich Fe-Si alloys at about 16 ($\pm$2) GPa. Crosses: bcc+hcp; open circles: hcp only; open squares: fcc+hcp; X:

fcc only; solid squares: bcc+fcc+hcp; open triangles: bcc+fcc; Tie lines indicate coexisting compositions in quenched samples that were analyzed by SEM. The experiments for Fe4.0wt%Si and Fe7.9wt%Si in a LVP were conducted at about 18 GPa and 14 GPa, respectively. For Fe7.9wt%Si alloy, two LHDAC experiments at 1387 K and 1501 K help establish the trend of the bcc+fcc phase region.

Web Figure Captions:

Web Figure 1 (A). Representative energy-dispersive x-ray diffraction patterns of Fe7.9wt%Si at 39 GPa upon heating. F: the fluorescence peak of Pb; e: Ge detector escape peak; b1: NaCl in b1 structure; b2: NaCl in b2 structure. NaCl was used as the thermal insulator and the pressure calibrant (13, 14). The sample was in the hcp structure at 39 GPa and 300 K. The hcp phase transformed to the bcc+hcp phases at 1324 K and, upon further heating, to bcc+fcc+hcp phases at 1999 K. **(B).** Representative angle-dispersive x-ray diffraction patterns of Fe7.9wt%Si at 76 GPa. A monochromatic beam (wavelength = 0.4246 Å) was used as the x-ray source. Re represents the rhenium gasket peak. The sample was in the hcp structure at 76 GPa and 300 K. The hcp phase transformed to the bcc+hcp phases at 1772 K and 1937 K.

Web Figure 2. Back-scattered electron image of the quenched LVP sample from 14.1 GPa and 1100 K. The Si contents of the bcc and fcc phases were presumably preserved by turning off the power supply at high pressure. Chemical analyses of the sample indicate that the bcc phase contains 10.3 ($\pm$0.1) wt% Si in dark areas and the fcc phase contains 6.7 ($\pm$0.1) wt% Si in bright areas. Black areas are the MgO matrix. As shown, no reaction between the sample and the MgO matrix was observed in a SEM. The white bar on the picture is 20 μm.

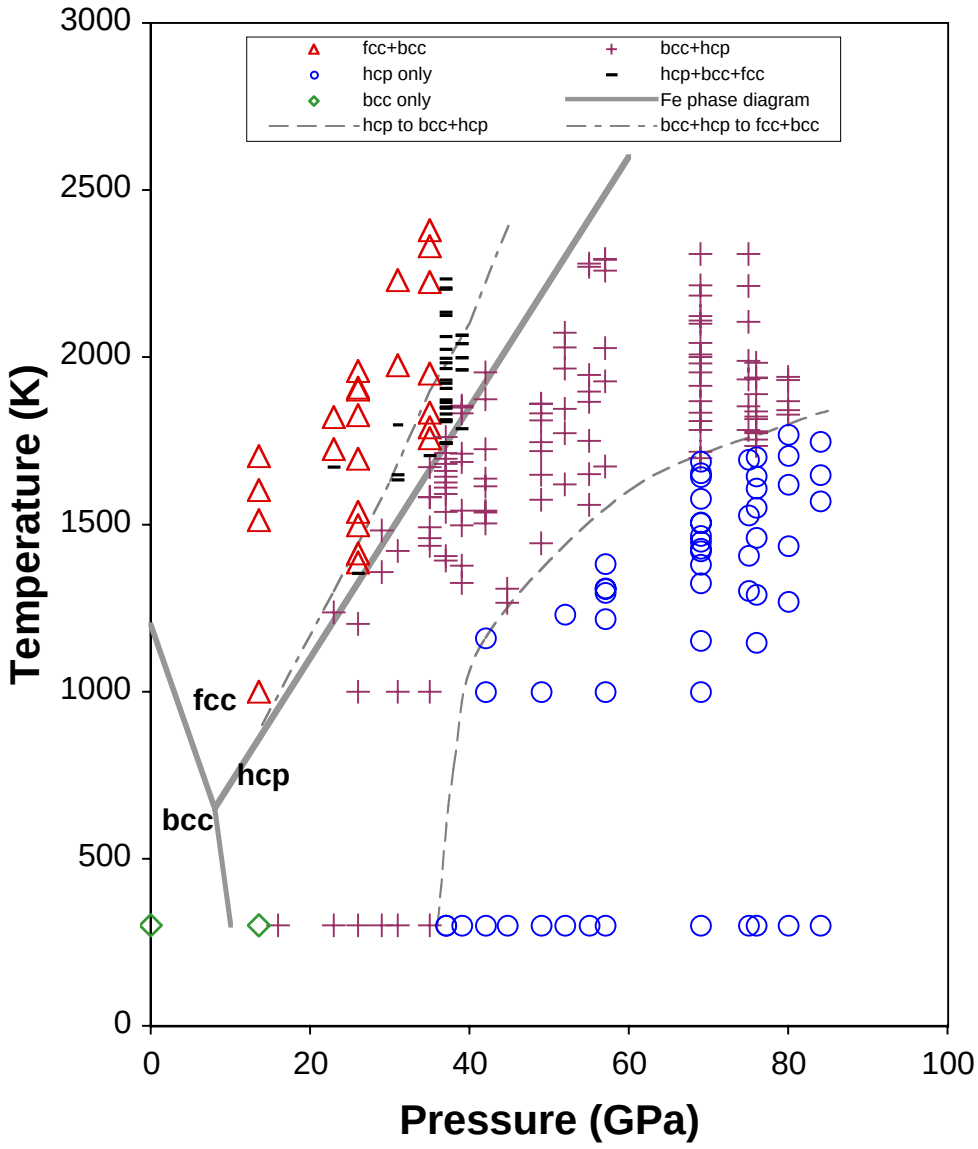
fcc+bcc
bcc+hcp
hcp only
hcp+bcc+fcc
bcc only
Fe phase diagram
hcp to bcc+hcp
bcc+hcp to fcc+bcc
fcc
hcp
bcc
Temperature (K)
Pressure (GPa)
0
500
1000
1500
2000
2500
3000
0
20
40
60
80
100

Figure 1

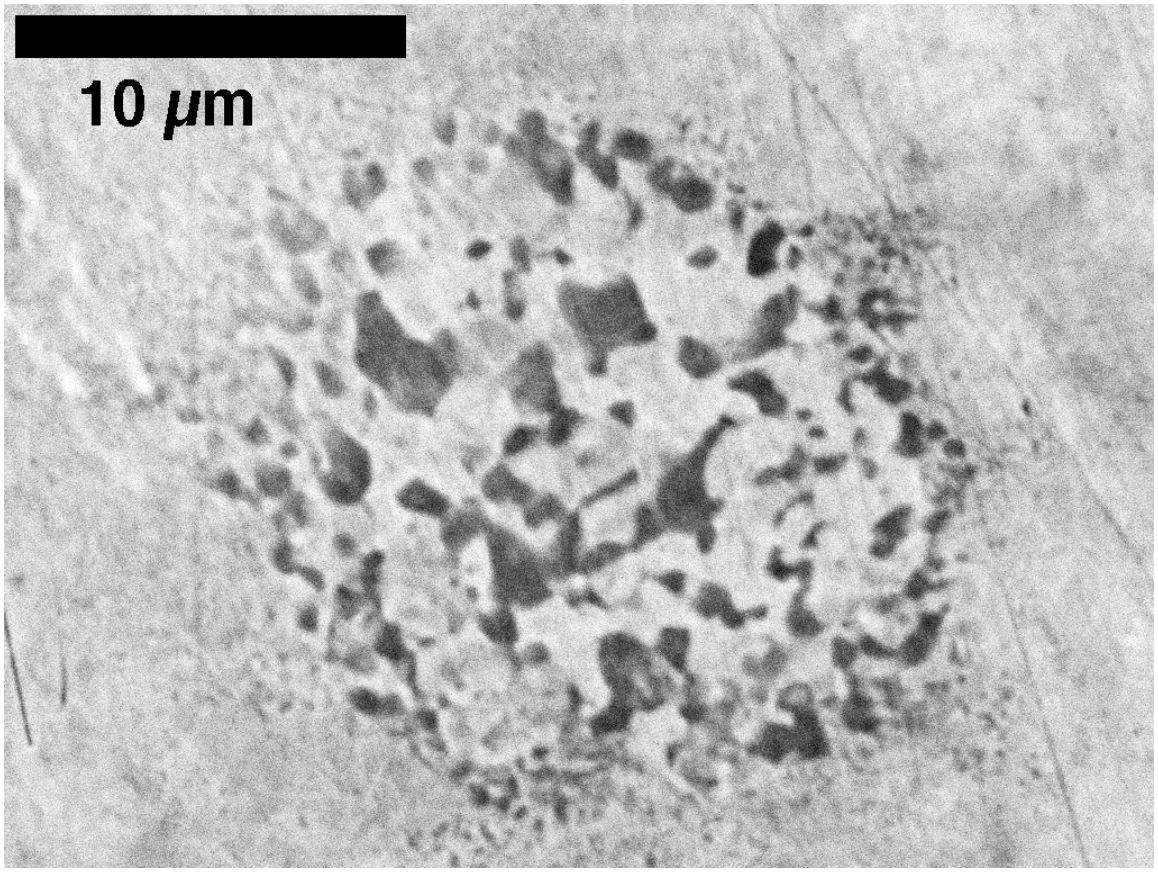

Figure 2

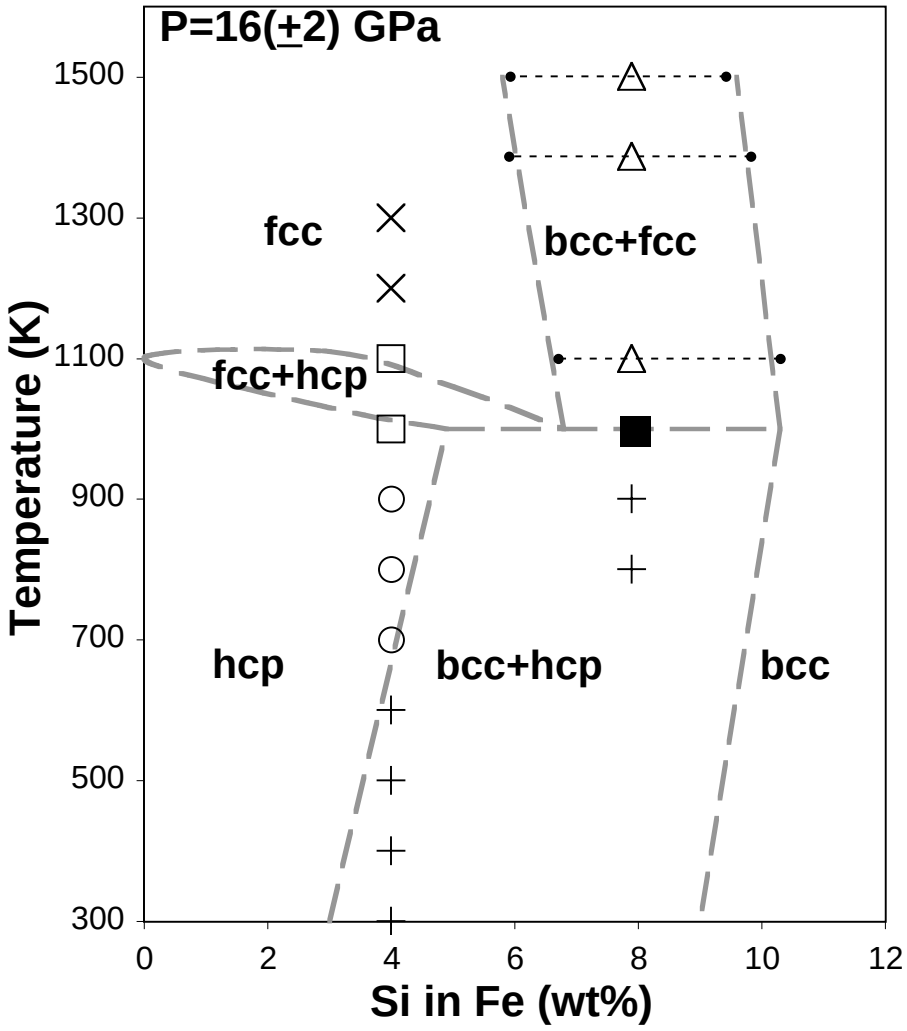
P=16(±2) GPa
1500
1300
1100
900
700
500
300
Temperature (K)
fcc
bcc+fcc
fcc+hcp
hcp
bcc+hcp
bcc
0
2
4
6
8
10
12
Si in Fe (wt%)

Figure 3

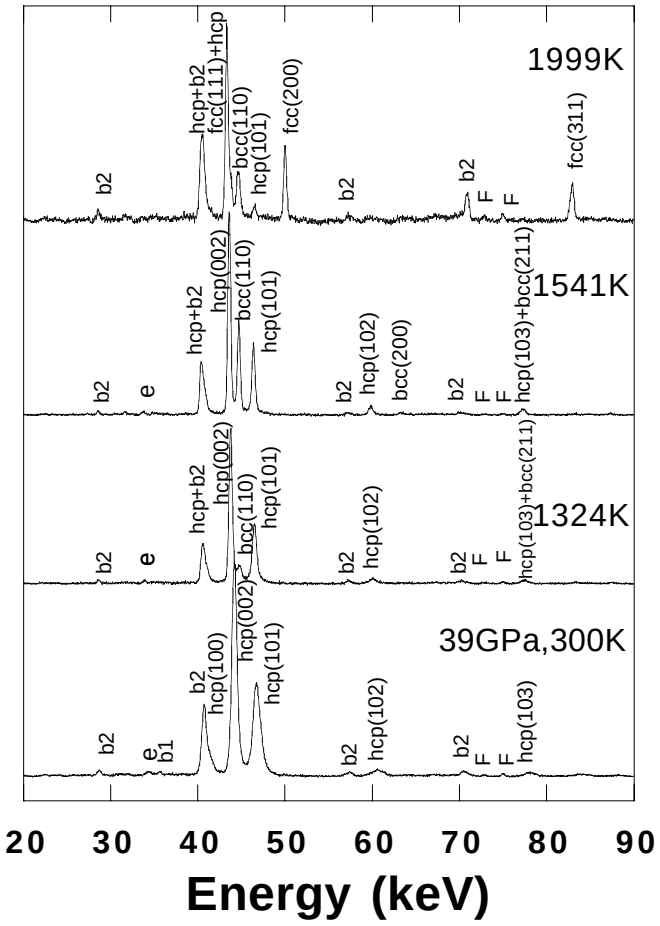

Web Figure 1A

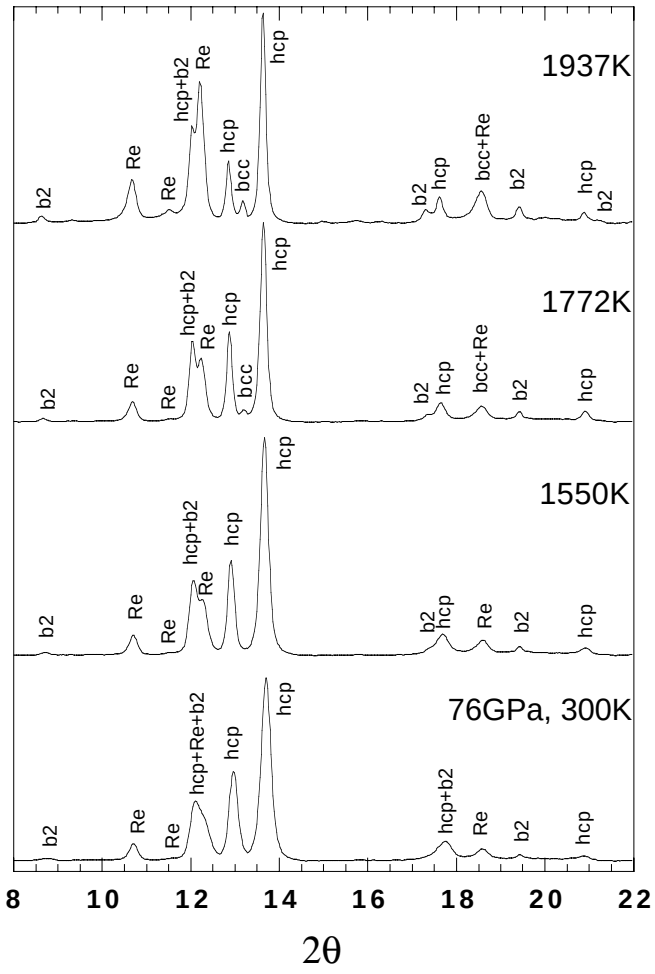

Web Figure 1B

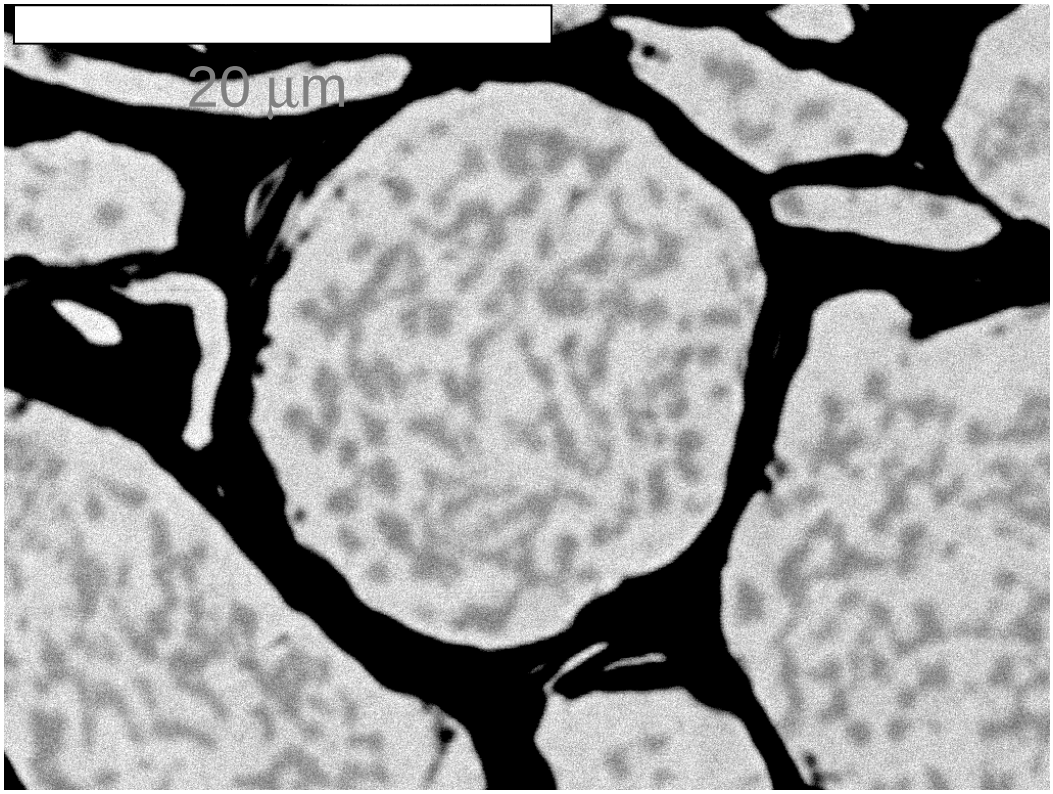

Web Figure 2